FDM Simulation of Broadband Seismic Wave Propagation in 3-D Heterogeneous Structure using the Earth Simulator

Project Representative

Takashi Furumura   Center for Integrated Disaster Information Research, Interfaculty Initiative in Information Studies / Earthquake Research Institute, The University of Tokyo

Authors

Shunsuke Takemura[*1], Takashi Furumura[*1, 2] and Takuto Maeda[*1, 2]

*1 Earthquake Research Institute, The University of Tokyo

*2 Center for Integrated Disaster Information Research, Interfaculty Initiative in Information Studies, The University of Tokyo

We conduct finite-difference method (FDM) simulation of broadband (f = 0.125-4 Hz) seismic wave propagation in southwestern Japan using the heterogeneous structure model including surface topography and small-scale velocity fluctuation in the crust and mantle. By the comparison of dense seismic observations and FDM simulations, we examine the effect of small-scale heterogeneities in the seismic wavefield. The observed seismogram envelope shape and longer duration coda waves are well reproduced by introducing surface topography to ordinary layered structure model, although the simulated spatial amplitude pattern and amplitude decay are not good agreement with observation. Heterogeneous structure model including both topography and velocity fluctuation in the crust and mantle can reproduce the observed seismic wave envelope shape, amplitude decay and maximum amplitude pattern.

Keywords: High-frequency seismic wave, heterogeneity, topography, scattering

1. Introduction

Broadband seismic wavefield including low-frequency to high-frequency (f > 1 Hz) seismic wavefields is very complicated, because the scattering of seismic waves due to small-scale heterogeneities in the crust and upper-mantle structure along the propagation path gradually dominates in the high-frequency seismic wavefield with frequencies over f > 1 Hz. Observed characteristics of the low-frequency (f < 0.5 Hz) wavefields can be reproduced by using the layered-structure model in which the large-scale structure is described by a number of layers with different velocity, density and attenuation parameters (e.g., Furumura et al., 2003)[1]. On the other hand, propagation features of the high-frequency (f > 1 Hz) seismic waves are completely different compared with those of low-frequency seismic waves due to the dominance of small-scale heterogeneities with shorter characteristic scale than wavelength of high-frequency seismic waves.

A few studies have demonstrated that the finite-difference-method (FDM) simulation of seismic wave propagation using a composite model including small-scale velocity fluctuation embedded over averaged layered-structure model can reproduce the observed characteristics of the high-frequency seismic waves very effectively (e.g., Nielsen et al., 2003 [2]; Furumura

and Kennett, 2005 [3], 2008 [4]; Kennett and Furumura, 2008 [5]). However, in these studies, the effect of the scattering of high-frequency waves due to surface topography was not examined. Kumagai et al. (2011)[6] may be an exception who recently conducted a numerical simulation for seismic wave propagation at Mt. Cotopaxi using a complex, realistic surface topography model with fluctuation of velocities in the structure. Through their simulations, Kumagai et al. demonstrated that the simulated high-frequency (f > 5 Hz) seismic wavefield is strongly influenced by both surface topography and velocity fluctuation in the subsurface structure.

In this report, we simulate broadband seismic wavefield including low- to high-frequency components using the heterogeneous layered-structure model including crust-mantle (Moho), mid-crust (Conrad) interfaces etc., and with surface topography and stochastic random velocity fluctuation in each layer. By the direct comparison of simulated and observed waveforms, we examine the effects of heterogeneities on the broadband seismic wavefields.

2. FDM simulation of broadband seismic wave propagation in 3-D heterogeneous structure

We conduct FDM simulation of seismic wave propagation in the Chugoku–Shikoku area of southwestern Japan to examine the effects of heterogeneous structures on the seismic wavefield by comparison of the simulated waveforms and the observations at seismic stations. Figure 1 shows the region of the FDM simulation and distribution of the broadband F-net, and strong motion K-NET and KiK-net stations. The model of FDM simulation is covering the zone 204.8 km by 204.8 km by 64 km, which is discretized by 0.1 km in horizontal direction and 0.05 km in vertical direction. To take the complex topography into account in the model, we employ a finer grid model in the vertical direction. The seismic wave propagation at each grid point in the elastic model is calculated by solving the equation of motion in 3-D based on the 4th order staggered-grid FDM in space and 2nd-order scheme in time (e.g., Graves, 1996) [7]. To conduct large-scale 3-D FDM simulations of seismic
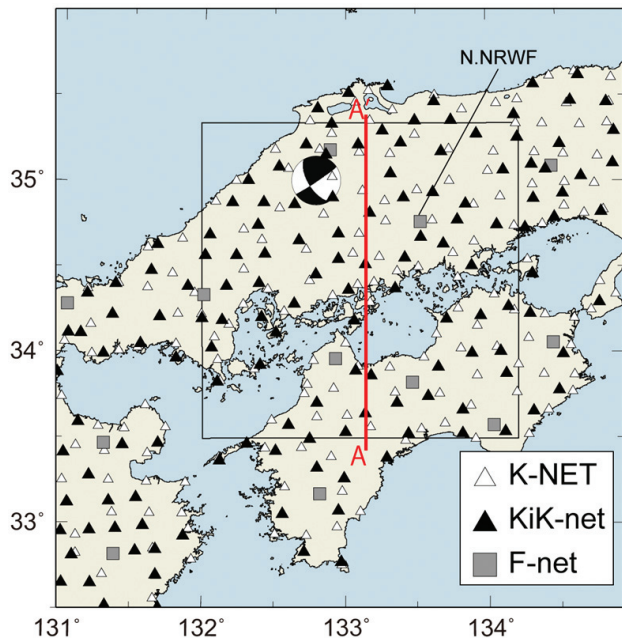
wave propagation, we employ a technique involving domain partitioning for parallel FDM using a large number of processors using a Message Passing Interface (MPI) for inter-processor communication (e.g., Furumura and Chen, 2004 [8], 2005 [9]).

The 3-D seismic velocity model used in this simulation is constructed according to the heterogeneous crust and upper-mantle structural models derived based on the receiver function studies (e.g., Shiomi et al., 2004 [10], 2007[11]) with the upper plane of the Philippine Sea plate and the Moho and Conrad discontinuities. The average P- and S-wave velocities, density, and attenuation (Q_P and Q_S) parameters of each layer are shown in Table 1. The minimum average S-wave velocity is V_S = 3.1 km/s. It is expected that the scattering and amplification of seismic wave due to variation in the very shallow layer, which has a depth of less than several ten meters beneath each station and S-wave velocity below V_S < 3.1 km/s, may be difficult to handle in the present FDM simulations. However, it is confirmed in the Chugoku-Shikoku area that the variation of the site amplification factors estimated by the coda-normalization method is not so strong to cause strong variation at each station as is often observed in compared northern Japan (Takemoto et al., 2011 [12]).

A complex topography model with a 50-m resolution provided by the Geospatial Information Authority of Japan is used in the present simulation. In order to achieve the precise simulation of high-frequency seismic scattering due to topography, we apply suitable boundary conditions for the irregular solid/air boundary for FDM simulation. Though the simulation of seismic wave propagation is conducted based on 4th-order staggered grid FDM, we use 2nd-order FDM across the solid/air boundary to realize accurate free-surface boundary condition (e.g. Maeda and Furumura, 2011)[13].

Small-scale velocity heterogeneities in the model are constructed by stochastic random velocity fluctuations in 3-D space $\xi(x,y,z)$ embedded over a uniform background velocity V_0, which is described as $V(x,y,z) = V_0[1+\xi(x,y,z)]$. The velocity fluctuation models for the crust and upper-mantle structure are stochastically characterized by an exponential-type PSDF with parameters of the correlation distance a = 5 km and rms strength ε = 0.05 in the crust, and a = 20 km and ε = 0.02 in the mantle

Fig.1 Model region and station distribution. Black triangle, white triangle, and gray square denote K-NET, Hi-net/KiK-net, and F-net stations, respectively. The squared region inside the map is the area of the FDM simulation of seismic wave propagation.

Table 1 Average background velocities, density, and attenuation coefficients in each layer.

Medium Column	V_P [km/s]	V_S [km/s]	ρ [kg/m^3]	Q_P	Q_S
Air	0.0	0.0	1.0	0	0
Upper crust	5.50	3.10	2600	300	300
	6.00	3.53	2700	680	400
Lower crust	6.70	3.94	2800	680	400
Mantle	7.80	4.60	3200	850	500
Philippine Sea plate	5.50	3.10	2600	300	300
	6.80	4.00	2900	510	300
	8.00	4.70	3200	850	500

(e.g. Saito et al., 2005 [14]; Takemura et al., 2009 [15]).

Figure 2 shows an example of the *S*-wave velocity structure along the cross-section from south to north of the simulation model, including homogeneous and heterogeneous crust and mantle structures, the shallowly dipping Philippine Sea plate, and irregular surface topography. Most present simulations of seismic wave propagation use layered structure model (Fig. 2a). Based on this, we introduced the surface topography (Fig. 2b) and velocity fluctuation (Fig. 2c) into the layered structure model. Such layered structure and surface topography are determined directly from geophysical and geological experiments, although the velocity fluctuations are not estimated directly from the experiments and so we assumed here stochastically.

The seismic source at the Shimane–Hiroshima boundary which occurred in May 13, 2007 at depth of 8 km is used in this study. Focal mechanism with strike/dip/rake = 56/86/152 and moment magnitude of M_w = 4.3 for this event is derived by a CMT solution provided by the F-net. To model the source
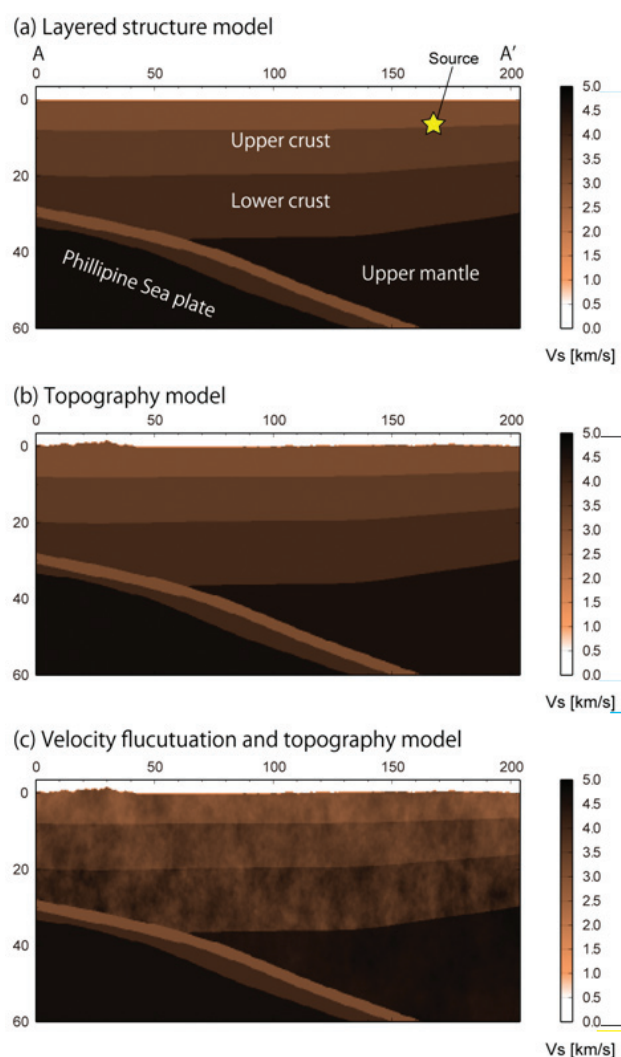
Fig.2 2-D vertical profiles of the *S*-wave velocity structure cross-section of the 3-D heterogeneous models along the path A-A' (Fig. 1). (a) Layered-structure model, (b) topography model, and (c) both velocity fluctuation and topography model.

rupture process of a small earthquake, we assume a normalized moment rate function that is represented by the asymmetric cosine function (Ji et al., 2003) [16] with dominant period 0.5 sec.

Through a set of experiments, we compare simulated waveforms with observed waveforms in the frequency range of 0.01–5 Hz, because it is found that the high-frequency components of the observed source spectrum drop below noise level over this frequency band.

3. Comparison of simulation results and dense seismic observations

The FDM simulation results for seismic wave propagation using various heterogeneous models are shown in Fig. 3 as paste ups of the radial-component velocity waveforms derived by the simulation using different structural models (Figs. 3b–d), and that of the observed Hi-net record (Fig. 3a) for frequency range from 0.125-4 Hz. Each trace of the seismogram paste up is multiplied by its hypocentral distance to compensate geometrical spreading factor of the body waves.

The observed waveforms shown in Fig. 3a show very much complicated properties with multiple reflected signals and long-duration *P*- and *S*-coda waves. On the other hand, the simulated waveform from the layered-structure model shown in Fig. 3b consists of a number of spiky signals for both *P* and *S* waves, with no clear coda waves generated following the body *P* and *S* waves. These spiky signals are developed by coherent multiple reflections of the direct *P* and *S* waves from each layer in the model. Such anomalous spiky signals developed by the layered model are weakened significantly by introducing the irregular topography at the top of the model as the incoherent multiple reflections disrupt the coherent pattern of multiple reflections, and also by enhancing the scattering of high-frequency seismic waves (Fig. 3c). The long-duration coda waves due to the scattering of seismic waves in the irregular topography also appear following direct wave arrivals. It is confirmed that the variation of the waveform amplitude at each station is very strong due to localized amplification of seismic wave caused by the surface topography in nearby stations. By adding the velocity fluctuation in each layer, the properties of the decay rate of wave amplitude with increasing epicentral distance match to the observations due to the loss of seismic energy by strong seismic wave scattering of high-frequency signals in the heterogeneous structure (Fig. 3d).

In order to compare the observed and simulated broadband waveforms derived by the FDM simulation using different structural models, including surface topography and velocity fluctuations, we compare the EW-component broadband (0.125-4 Hz) velocity waveforms recorded at the F-net station of N.NRWF at hypocentral distance of 73 km between simulations and observation. Figure 4 shows the observed and simulated seismograms of EW component recorded at N.NRWF. For the

observed F-net waveform (Fig. 4a), the amplitude of *P* wave is slightly less than later *S*-wave amplitude. However, the simulated waveforms derived from the layered structure model (Fig. 4b) and topography model (Fig. 4c) show much larger and impulsive *P*-wave signal in the EW component compared with observation. By introducing velocity fluctuation in the simulation model (Fig. 4d), the *P*-wave amplitude clearly decrease compared with other two models. It is indicating that the cause of amplitude decay of *P* wave may be the seismic wave scattering due to velocity fluctuation along propagation

(a) Observation

(b) Layered structurre model
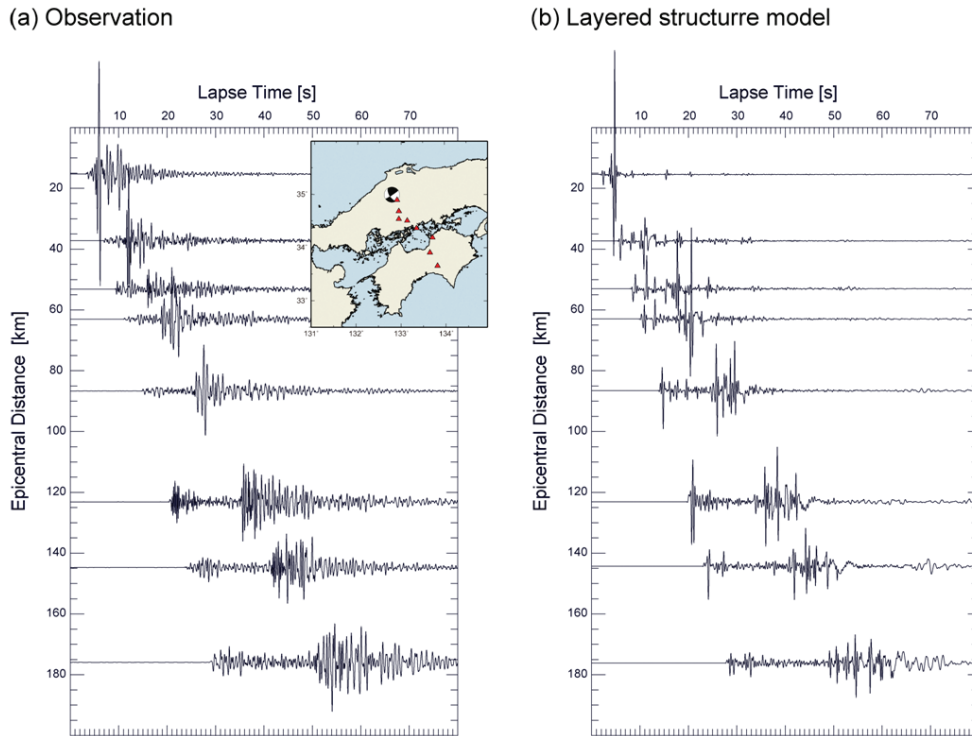
Fig. 3 Comparison of the observed and simulated waveforms of radial component velocity motion for broadband (0.125-4 Hz) waveforms. (a) Observed waveforms at Hi-net stations and (b) simulated waveforms using the layered-structure model. Each trace is multiplied by hypocentral distance to compensate geometrical spreading.

(c) Topography model

(d) Velocity fluctuation and topograhy model
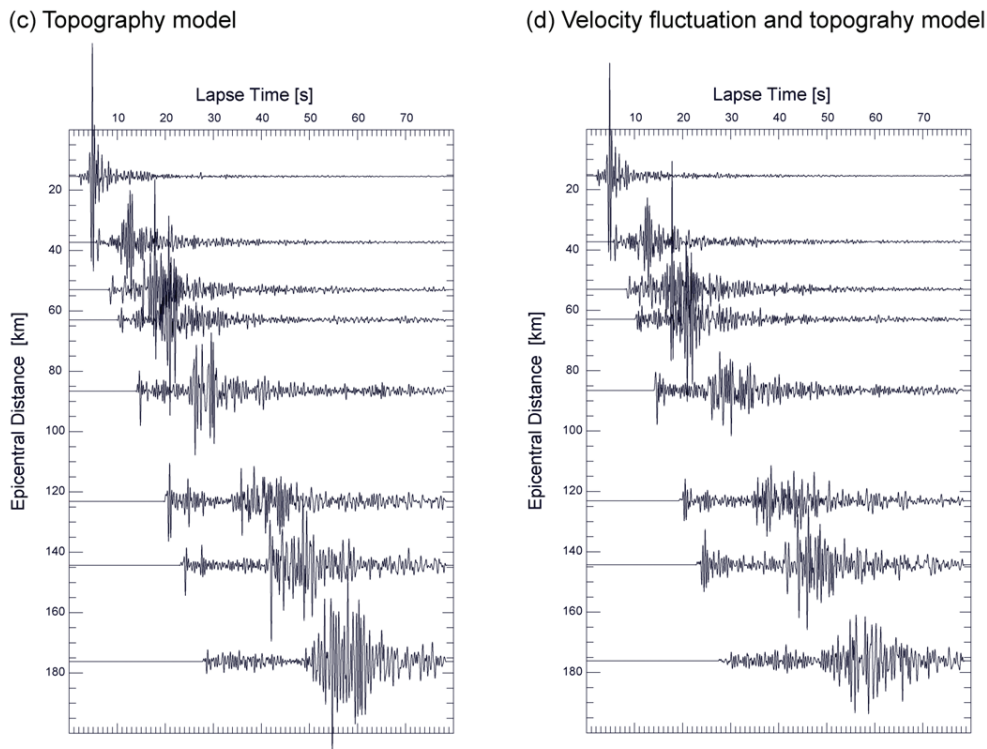
Fig. 3 (continued) (c) simulated waveforms using the topography model and (d) both velocity fluctuation and topography model.

88

(a) Observed waveform

(b) Layered structure model

(c) Topography model

(d) Velocity fluctuation and topography model
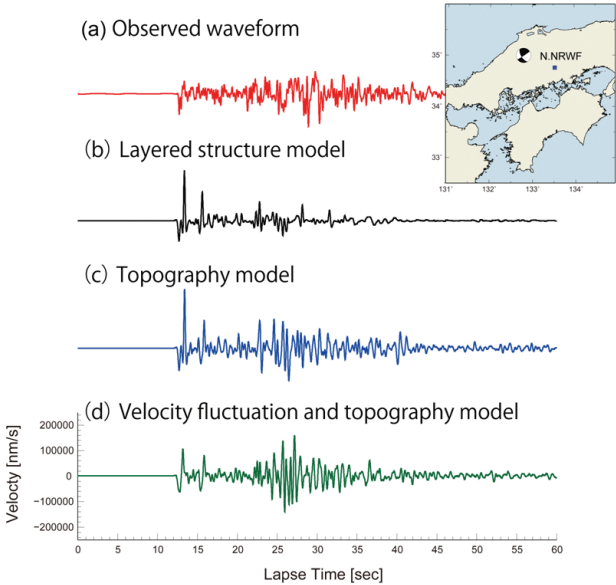
Fig. 4 Comparison of simulated and observed broadband (f = 0.125-4 Hz) seismic waves of EW component recorded at N.NRWF station (Fig. 1).

path. FDM simulation in the layered structure model with topography and suitable velocity fluctuation can reproduce the observed waveform shape, direct-wave duration, later coda excitation and amplitude ratio.

In the case of homogeneous medium, it is theoretically predicting that the spatial amplitude pattern of S wave is showing four-lobe pattern. However, some studies demonstrated that in high frequency ($f > 1$ Hz), the spatial pattern of maximum S-wave amplitude shows almost isotropic pattern (e.g. Takemura et al., 2009)[15]. Here, we examine the spatial pattern of the peak ground velocity for the high-frequency band derived by the simulation using different structural model and observation. Figure 5 shows the spatial distribution of maximum S-wave amplitude of the ground velocity examined at the K-NET and the KiK-net strong motion stations. The resultant pattern of ground motions derived from the simulation of the layered-structure and topography models maintain the four-lobe portion of the S-wave radiation pattern for the strike-slip fault source (Figs. 5a, b). However, in the simulation result, including both velocity fluctuation and topography model (Fig. 5c), the
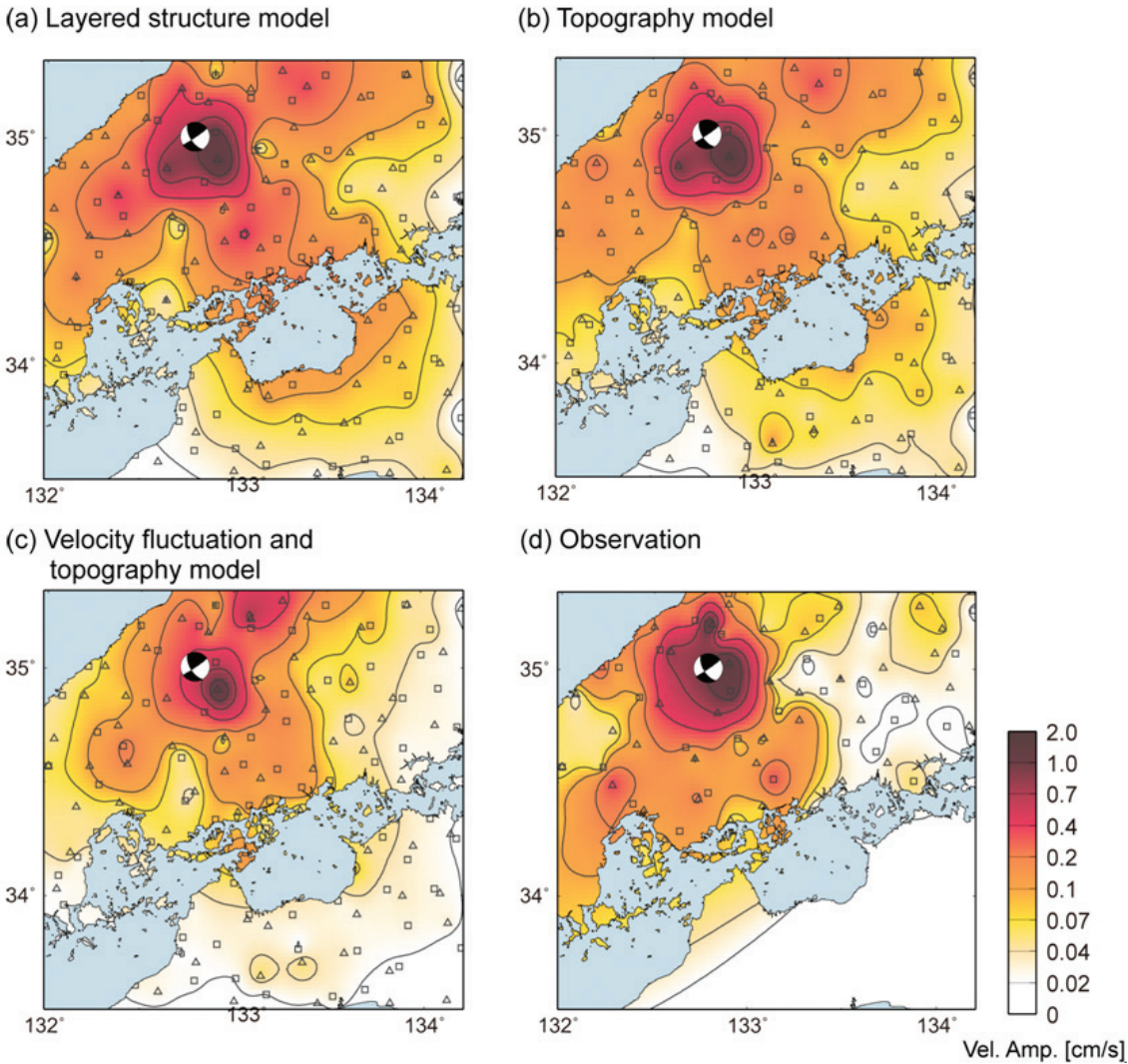
Fig.5   Comparison the maximum S-wave amplitude distribution in the high-frequency ($f > 1$ Hz) band derived from (a-c) simulation using different heterogeneous model and (d) observation at K-NET and KiK-net station at free surface.

pattern is considerably distorted, showing almost isotropic pattern at longer distances, which is almost comparable with observations (Fig. 5d). However, the observed amplitude pattern shows a more complicated pattern that may be caused by other heterogeneities, such as site amplification, mesoscale heterogeneities, and source rupture processes.

4. Conclusion

We conducted FDM simulations of broadband seismic wave propagation using ordinaly layered structure model with realistic surface topography and small-scale velocity fluctuation in order to construct the heterogeneous structure model which can explain characteristics of complex observed seismic wavefield.

The ordinaly layered structure model can not reproduce complex fetures of the observed broadband seismic wavefield. By introducing surface topography and suitable small-scale velocity fluctuation models in the model, complex body waves and longer duration coda waves appear in simulated seismograms. However, the observed maximum amplitude pattern and amplitude decay derived from the simulation in the model with topography alone don't have good agreements with observations. One of the causes of this discrepancy between observation and simulation in the model with toporaphy alone is the scattering properties of seismic waves on the surface topography, which seismic wave scattering due to topography occurs on the free surface only. Simulation results derived from both velocity fluctuation and topography model match to the observed maximum amplitude pattern and amplitude decay because of strong seismic scattering due to small-scale velocity fluctuation along propagation path.

For estimating strong ground motion disaster associated with larger earthquakes, the contribution of the site amplification effect due to shallow low-velocity layers is also very important. Therefore, in the feature, we should consider such site effect on the high-frequency seismic wave to achive more practical strong motion prediction for feature large eathquakes.

Acknowledgements

References

[1] T. Furumura, K. Koketsu, and B. L. N. Kennett, "Visualization of 3D wave propagation from the 2000 Tottori-ken Seibu, Japan, earthquake: observation and numerical simulation" Bull. Seismol. Soc. Am., 93, pp.870-881, 2003.

[2] L. Nielsen, H. Thybo, A. Leavander, and L. N. Solodilov, "Origin of upper-mantle seismic scattering-evidence from Russian peaceful nuclear explosion data" Geophys. J. Int., 154, pp.196-204, 2003.

[3] T. Furumura and B. L. N. Kennett, "Subduction zone guided waves and the heterogeneity structure of the subducted plate: intensity anomalies in northern Japan" J. Geophys. Res., 110, pp.B10302, 2005.

[4] T. Furumura and B. L. N. Kennett, "A scattering waveguide in the heterogeneous subducting plate" Advances in Geophysics, Scattering of Short-Period Seismic Waves in Earth Heterogeneity, Eds. H Sato and M. Fehler, Elsevier, 50, Chap.7, pp.195-217, 2008.

[5] B. L. N. Kennett and T. Furumura, "Stochastic waveguide in the lithosphere: Indonesian subduction zone to Australian craton" Geophys. J. Int., 172, pp.363-382, 2008.

[6] H. Kumagai, T. Saito, G. O'Brien, and T. Yamashita, "Characterization of scattered seismic wavefields simulated in heterogeneous media with topography" J. Geophys. Res., 116, pp.B03308, 2011.

[7] R. W. Graves, "Simulating seismic wave propagation in 3D elastic media using staggered-grid finite differences" Bull. Seismol. Soc. Am., 86, pp.1091-1106, 1996.

[8] T. Furumura and L. Chen, "Large scale parallel simulation and visualization of 3D seismic wavefield using Earth Simulator" CMES, 6, pp.153-168, 2004.

[9] T. Furumura and L. Chen, "Parallel simulation of strong ground motions during recent and historical damaging earthquakes in Tokyo, Japan" Parallel Computing, 31, pp.149-165, 2005.

[10] K. Shiomi, H. Sato, K. Obara, and M. Ohtake, "Configuration of subducting Philippine Sea plate beneath southwest Japan revealed from receiver function analysis based on the multivariate autoregressive model" J. Geophys. Res., 109, pp.B04308, 2004.

[11] K. Shiomi, M. Matsubara, Y. Ito, and K. Obara, "Simple relation between seismic activity along Philippine Sea slab and geometry of oceanic Moho beneath southwest Japan" Geophys. J. Int., 173, pp.1018-1029, 2008.

[12] T. Takemoto, T. Furumura, T. Saito, T. Maeda, and S. Noguchi, "Spatial- and Frequency-dependent properties of site amplification factors in Japan derived from coda normalized method" Bull. Seismol. Soc. Am., in press, 2012.

[13] T. Maeda and T. Furumura, "FDM simulation of seismic

waves, ocean acoustic waves, and tsunami based on tsunami-coupled equation of motion" Pure Appl. Geophys., published online, doi:10. 1007/s00024-011-0430-z, 2011.

[14] T. Saito, H. Sato, M. Ohtake, and K. Obara, "Unified explanation of envelope broadening and maximum amplitude decay of high-frequency seismograms based on the envelope simulation using Markov approximation: Forearc side of the volcanic front in northeastern Honshu, Japan" J. Geophys. Res., 110, pp.B01304, 2005.

[15] S. Takemura, T. Furumura, and T. Saito, "Distortion of the apparent S-wave radiation pattern in the high-frequency wavefield: Tottori-Ken, Seibu, Japan, earthquake of 2000" Geophys. J. Int., 178, pp.950-961, 2009.

[16] C. Ji, D.V. Helmberger, D.J. Wald, and K.F. Ma, "Slip history and dynamic implication of the 1999 Chi-Chi, Taiwan, earthquake" J. Geophys. Res., 108, pp.2412, 2003.

地球シミュレータによる３次元不均質媒質中を伝播する広帯域地震動シミュレーション

プロジェクト責任者

古村　孝志　　東京大学　大学院情報学環総合防災情報研究センター

　　　　　　　東京大学　地震研究所

著者

武村　俊介 [*1]，古村　孝志 [*1, 2]，前田　拓人 [*1, 2]

*1　東京大学　地震研究所

*2　東京大学　大学院情報学環総合防災情報研究センター

　西南日本を対象として、小さなスケールの速度不均質構造と実際の地表面形状を含んだ構造モデルを用いて差分法による広帯域地震動シミュレーションを行った。高密度な地震観測網で得られた観測記録とシミュレーション波形を比較することで、それぞれの不均質構造が地震波動場におよぼす影響を検討した。その結果、地形や速度ゆらぎなどの短波長不均質構造による地震波散乱によって、観測波形に見られる複雑な実体波や Coda 波が励起していることが明らかとなった。但し、地形のみを考慮したモデルでは最大振幅の空間分布や距離減衰の様子を再現することができず、速度ゆらぎと表層地形の双方を仮定することによって、観測される地震動の包絡線形状、最大振幅の空間変化を再現することができた。

キーワード：地震, 高周波数地震動, 不均質構造, 地形, 地震波散乱

地球シミュレータによる３次元不均質媒質中を伝播する広帯域地震動シミュレーション